No plate tectonics in the Eoarchaean at Isua

Hugh Rollinson

School of Built and Natural Environment, University of Derby,

Kedleston Road, Derby, DE22 1GB, UK

h.rollinson@derby.a.c.uk

Supplemental Material

1. DATA SOURCES FOR REE AND TH-NB PLOTS

The REE and Nb-Th data used in this study were taken from the studies by

Polat et al., (2002)

Polat et al., (2003)

Polat and Hofmann (2003)

Jenner (2009)

Furness et al., (2009)

Hoffmann et al., (2011)

Rizo et al. (2011)

Rizo et al. (2013)

Szilas et al. (2015)

O'Neil et al. (2016)

Saji et al., (2018).

A small amount of REE data for metabasalts from the Eastern limb of the greenstone belt is also given in Komiya et al (2004). These appear to include boninite-like and tholeiitic samples described respectively as MORB- and OIB-like. However, there are few data and the OIB-like samples appear to have an unusual negative Gd-anomaly which is presumed to be analytical error. These data were not included in the current dataset.

2. RARE EARTH ELEMENT MOBILITY

Some previous authors have documented the fact that the light REE and the isotopes of Nd have been mobile in the Isua metabasites, in part due to their subsequent metamorphism both in the Eoarchaean and in the Neoarchaean (Frei et al., 2002; Rollinson 2003). Detailed geochemical studies by Polat et al., (2002; 2003) showed that some Isua metabasites have experienced post magmatic chemical change. Normally the REE are thought to be excluded from this process but it is clear that at Isua this is not the case. Further evidence for Nd mobility comes from studies of Nd isotopes. A recent example being the work of Rizo et al. (2011) who showed that some metabasalts from the western arm of the Isua Belt defined a 3.7 Ga ^{147}Sm-^{143}Nd isochron, whereas other samples from the same area defined a 2.9 Ga isochron.

For this reason, the database used in this study has been carefully screened to eliminate samples in which the REE may not be primary. For example, only the undisturbed samples of Polat et al. (2002; 2003) and Rizo et al., (2011) have been used. Elsewhere samples with very high light REE concentrations have been carefully examined. Previous studies suggest that light REE mobility maybe associated with higher P_2O_5 in the rock (Polat et al., 2011). Support for this view comes from unpublished SEM observations which show fractures in garnet grains in metapelites from the same area as the metabasites, which are enriched in light REE-rich phosphates. Thus, samples with high light REE and high P_2O_5 (normally > 0.1 wt % P_2O_5) were eliminated from the database. This means that highly LREE enriched samples previously described from these rocks are here regarded as the product of element mobility and of no petrological significance. This disturbance may also have a bearing on the variable ^{142}Nd signal recorded in these rocks and discussed recently by Saji et al. (2018). It is argued here therefore that the results in the screened sample set used in this study are robust, for they display a consistent similarity in the groups of REE patterns found and in the repeatable ^{143}Nd isochron ages.

3. MODELLING OF THE REE

The *PM source* used here is that of Palme and O'Neill (2014), chondrite normalised using the values of Barratt et al. (2012). Melting of this source to generate tholeiites with light-enriched REE patterns with La/Yb_N=1.6-4.1 assumed a mineral assemblage of 50% olivine, 40 orthopyroxene, 8% clinopyroxene, 2% spinel, 10-15 % batch melting and up to 30% olivine fractionation. The REE partition coefficient data are from Rollinson and Pease (2021).

The composition of the *lower mantle source* was calculated as follows:

(a) Starting with the PM composition a depleted mantle composition was estimated for the REE using the shape of the modern DM REE curve from Workman and Hart (2005) but element concentrations close to PM and adjusted so that $(Sm/Nd)_N \sim 1.1 \sim {}^{147}Sm/{}^{144}Nd = 0.22$. This estimate is used for the REE composition of the 4.39 Ga super-chondritic mantle.

(b) This composition was used as the starting composition for bridgemanite (Mg-perovskite) and Ca-perovskite fractionation using REE partition coefficient data from Corgne et al (2005), see Table 1. The fractionating assemblage was Ca:Mg 3:97. The calculated residue after 3% melt removal gives a depleted mantle with middle- and heavy-REE concentrations similar to PM and super-chondritic. It should be noted that recent work by Deng and Stixrude (2021) and Tateno et al. (2018) have shown that the partition coefficients for Hf and Sm-Nd are dependent on pressure although are similar in the pressure range examined by Corgne et al (2005) (20-25 GPa) and so do not detract from the present model.

(c) The melting of this source in the shallow mantle can generate tholeiites with light REE depleted patterns. The model assumes 20 % batch melting with the mineral assemblage: 50% olivine, 45% orthopyroxene, 5% clinopyroxene, followed by up to 40% olivine fractionation. The REE partition coefficient data are from Rollinson and Pease (2021).

Tholeiites with flat REE patterns were modelled using a refertilised source, based upon the depleted mantle source described above. In this case the depleted lower mantle source was refertilised with 4% of a 10% batch melt of the PM assuming a mineral assemblage of 50% olivine, 40 orthopyroxene, 8% clinopyroxene, 2% spinel. This refertilised source experienced 15-20% melting assuming a mineral assemblage of 50% olivine, 40 orthopyroxene, 8% clinopyroxene, 2% spinel, followed by up to 40% olivine fractionation.

^{142}Nd isotopic constraints on the source of the boninite-like basalts require an early depleted source and from the coupled εHf-εNd trend garnet fractionation in the source. The REE content of an appropriate source can be modelled using the residue from 5% majorite-garnet fractionation (using the partition coefficients of Corgne and Wood (2004), see Table 1).

30% batch melting of this source with equal amounts of olivine and orthopyroxene in the residue yields ultra-depleted melts. The mixing of these ultra-depleted melts in the range 0.5-10% with a 3% batch melt of PM, with 50% olivine, 40% orthopyroxene and 10% clinopyroxene in the residue yields a range of REE patterns from ultra-depleted to U-shaped. In this case modelling showed that it is more likely that the mixing was between melts and not the re-fertilisation of an ultra-depleted source.

The degree of refertilisation in the boninite-like basalts is measured using the light REE content which increases from the ultra-depleted source to the most refertilised. Using the data from Polat (2002) it can be seen that Ce (indicative of the light REE) correlates positively with SiO_2 and negatively with MgO. This indicates that the refertilisation process increases the silica content of the melt and dilutes the MgO content indicating that the migrating melt is silica-rich and MgO-poor relative to the parent ultra-depleted melt.

Hoffmann et al. (2011) in their study of tholeiitic basalts from Isua show an inflexion at MgO=10 wt% in their variation diagrams. This suggests that clinopyroxene fractionation (+/- plagioclase) occurs at <10 wt% MgO and olivine fractionation occurs at >10 wt% MgO. Many of the basalts in this study have MgO > 10 wt% and so have experienced only olivine fractionation/ accumulation, but there is a proportion that have MgO< 10 wt% and may therefore have also experienced clinopyroxene +/- plagioclase fractionation. The impact of clinopyroxene fractionation is to reduce the range of total REE and increase the La/Yb_n ratio. This is relevant to those samples that show enriched REE patterns. Of these, half the samples have MgO>10% and experienced olivine fractionation/ accumulation, whereas the other half may in part show enriched REE due to clinopyroxene fractionation. However, if clinopyroxene is accompanied by plagioclase this effect will be much reduced.

	Ca-Pvk	Mg-Pvk	Maj-grt
	C-2005	C-2005	CW-2004
La	10.0	0.006	0.020
Ce	11.0	0.015	0.025
Pr	13.0	0.013	0.029
Nd	15.0	0.018	0.043
Sm	20.0	0.050	0.095
Eu	22.0	0.081	0.150
Gd	21.5	0.125	0.188
Tb	21.0	0.200	0.280
Dy	20.5	0.300	0.398
Ho	20.0	0.380	0.507
Er	19.5	0.470	0.643
Tm	18.0	0.600	0.761
Yb	14.0	0.730	0.918
Lu	11.0	0.905	1.029
Nb	0.275	0.215	0.024
Th	16.0	0.006	0.017

Table 1. Partition coefficients used in this study for lower mantle phases. Ca-Pvk – calcium perovskite, Mg-Pvk -magnesium perovskite, Maj-grt - majorite garnet. Sources C-2005 = Corgne et al. (2005), CW 2004 = Corgne and Wood (2004). The Ca-Pvk values are based on the median of the higher range of values except for La which is raised in line with the other light REE. The Mg-Pvk values are the median for the range. Some REE are interpolated.

4. MODELLING NB/YB-TH/YB RATIOS

In detail the 3.8 Ga tholeiites (Th/Nb=0.08-0.45) plot away from the PM whereas the 3.7 Ga tholeiites (Th/Nb=0.147-0.942) plot on a similar trend away from a slightly depleted PM source. Samples with Th concentrations < 0.05 ppm were not used.

The steep trends on Nb/Yb vs Th/Yb plots imply that during mantle melting in the IGB Th behaves more incompatibly than Nb. Examination of partition coefficient data show that the controlling phase could be spinel, for partition coefficients have been reported for Nb in spinel of up to 0.86 (see data of Klemme et al. 2006 for lunar basalts). This is consistent with melting in the spinel stability field – ie within the shallow upper mantle.

Figure 2 of the main paper shows the results of trace element modelling for the PM source, a fractionated 4.39 Ga depleted mantle source and a 30% melt of an ultra-depleted source. Partition coefficient data are from Rollinson and Pease (2021). 3-30% batch melting of a PM source with the phases olivine (46-50%), orthopyroxene (40-44%), clinopyroxene (4%) and spinel 2-10% in the residue yields melts with the Nb/Yb and Th/Yb ratios shown as the red curves and representative of IGB tholeiites with high Nb/Yb ratios. Black crosses show melt fractions.

A 4.39 Ga fractionated depleted mantle source, as calculated for the REE using the perovskite partition coefficient data of Corgne et al (2005) has 0.26 ppm Nb (PM=0.595), 0.054 ppm Th (PM=0.085). 3-30% batch melting of this source with the phases olivine (46-50%), orthopyroxene (40-44%), clinopyroxene (4%) and spinel 2-10% in the residue yields melts with the Nb/Yb and Th/Yb ratios shown as the blue curves and representative of IGB tholeiites with low Nb/Yb ratios.

An ultra-depleted source, calculated as discussed above for the REE has Nb=0.035 ppm and Th=0.0033 ppm. A 30% melt of this source has Nb=0.114 ppm, Th=0.011 ppm. Olivine fractionation does not change the ratios.

5. HF-ND ISOTOPE SYSTEMATICS AND A DEPLETED HF-ISOTOPE MANTLE RESERVOIR

Figure 1 shows a compilation of εNd(t) vs εHf(t) plot for IGB basalts:

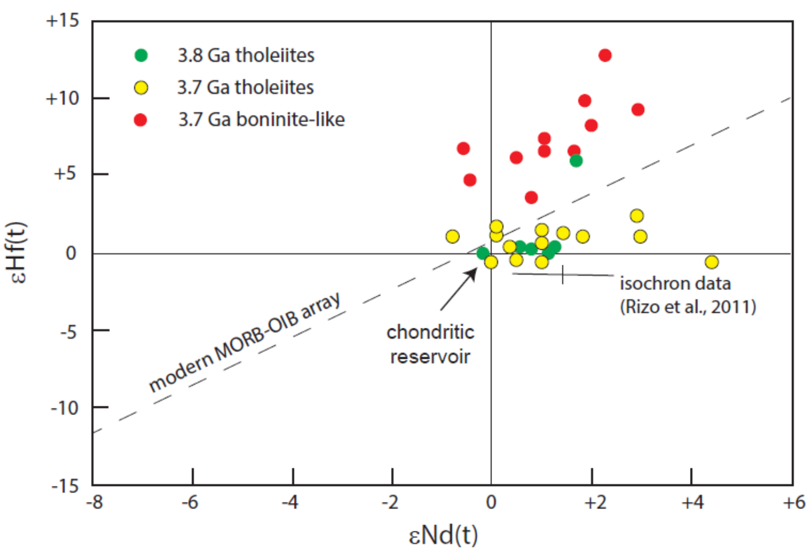

Figure 1. Compilation of εNd(t) vs εHf(t) plot for IGB basalts relative to the modern MORB-OIB array. Data from Hoffmann et al. (2011) and isochron data for 3.7 Ga tholeiites from Rizo et al. (2011).

A serious concern about the validity of a Hf-depleted mantle reservoir with a super-chondritic Lu/Hf ratio at 3.7 Ga has been raised from the study of Hf in Eoarchaean zircons. All zircons of this age show evidence of only a chondritic mantle source (Fisher and Vervoort, 2018; Kemp et al., 2019). However, it is important to note that the Eoarchaean zircons examined are in felsic rocks, which have been derived (most probably) from a tholeiitic basaltic source. It is very likely that the relatively rare boninite-like basalts were not sufficiently fertile to yield felsic melts containing zircon and so zircons derived from a Hf-depleted mantle reservoir are rarely represented in the zircon record (Hoffmann et al., 2014). It is important therefore to also consider the evidence for a depleted mantle reservoir from mafic and ultramafic rocks. For example, the trace element patterns in the boninite-like basalts show very clear evidence of being derived from an ultra-depleted mantle source at 3.7 Ga. Support for an Eoarchaean supra-chondritic εHf reservoir also comes from the ca 3.8 Ga mafic and ultramafic rocks of the Nulliak suite in northern Labrador (Morino et al., 2018) and the > 3.8 Ga ultramafic rocks found as enclaves in the Itsaq gneisses south of Isua (van de Locht et al, 2020).

6. CHALLENGES TO THE INTRA-MANTLE MODEL

It has been suggested, on the basis of sulphur isotope evidence that the Isua metabasalts have 'seen' a crustal source (Siedenberg et al. 2016). These rocks contain a small signature indicative of mass independent sulphur isotope fractionation (MIF) - $\Delta^{33}S$ = 0.17 to +0.26‰, average +0.02 ± 0.12‰ relative to the notional mantle value of 0‰. The MIF signal derives from atmospheric processes and so indicates the presence of crustal material in the mantle source. However, the size of the MIF signal measured thus far is so close to that of the mantle value that it is considered impossible to discriminate.

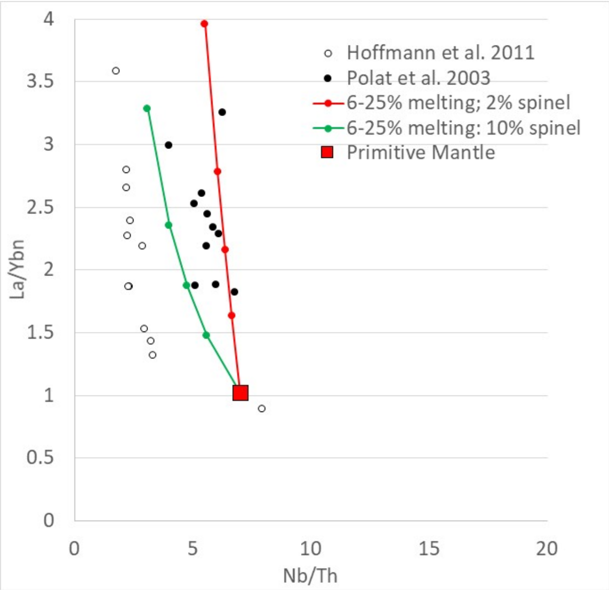

Figure 2. Nb/Th vs La/Yb$_n$ plot showing data for enriched tholeiites from Isua from Hoffmann et al. (2011) and Polat et al. (2003). Two calculated curves are shown for 6-25% batch partial melting of a primitive mantle composition with the mineralogy of a spinel lherzolite with compositions between olivine (46-50%), orthopyroxene (40%), clinopyroxene (4-8%), spinel (2-10%). Spinel partition coefficients were REE=0, Nb=0.86, Th=0.02. These parameters are consistent with the REE and Nb-Th models used for the origin of the enriched tholeiites elsewhere in this paper.

Further evidence for a crustal component was presented by Hoffmann et al. (2011) who argued from trace element concentrations that the enriched tholeiites were contaminated with a crustal component using trace element ratio diagrams such as La/Yb_n vs Nb/Th. However, it is shown here that when a wider data set is used for enriched tholeiitic basalts (ie to include the data of Polat et al. 2003) the data can be explained through different degrees of partial melting of a primitive mantle source (Figure 2) and does not require a crustal component.

7. HEAT-PIPES AND MANTLE PLUMES

The term heat-pipe was popularised by Moore and Webb (2013) who argued that in a rapidly cooling planet, such as the Hadean Earth, heat and material are transferred to the surface by localised channels known as heat-pipes. This is thought to be the dominant mode of planetary heat transport when heat production rates are high and gives rise to extensive volcanic resurfacing.

In contrast plumes are a product of mantle convection for their function is to remove excess heat from the core-mantle boundary (CMB). The main way in which this is done is to deliver large volumes of cold material to the CMB. In the absence of plate tectonics, it is unlikely that this occurs, and so plumes are not expected to be present prior to the onset of plate tectonics. Instead, a slow, passive upwelling occurs throughout the mantle in the form of heat-pipes. This global melting regime is the heat-pipe regime. Heat-pipes also short-circuit the thermal resistance of the lithosphere which subsequently becomes thicker as it transports less heat. It is important to note that in this study we have no data to suggest that the deeply sourced melts arose from as deep in the mantle as the CMB.

ADDITIONAL REFERENCES

Barrat, J.A., Zanda, B., Moynier, F., Bollinger, C., Liorzou, C., Bayon, G., 2012. Geochemistry of CI chondrites: Major and trace elements, and Cu and Zn Isotopes. Geochimica et Cosmochimica Acta v. 83, p. 79-92.

Corgne, A., Liebske, C., Wood, B.J., Rubie, D.C., Frost, D.J., 2005. Silicate perovskite-melt partitioning of trace elements and geochemical signature of a deep perovskitic reservoir Geochimica et Cosmochimica Acta, v. 69, p. 485–496,

Corgne A., Wood B. J. (2004) Trace element partitioning between majoritic garnet and silicate melt at 25 GPa. Phys. Earth Planet. Inter., v. 143–144, p. 407–419

Deng, J., Stixrude, L., 2021. Deep fractionation of Hf in a solidifying magma ocean and its implications for tungsten isotopic heterogeneities in the mantle. Earth Planet. Science Letters, 562, 116873.

Frei, R., Rosing, M., Waight, T.E., Krogstad, E.J., Storey, M., Ulfbeck, D.G., Albarède, F., 2002. Hydrothermal-metasomatic and tectonothermal processes in the Isua greenstone belt (West Greenland): a multi-isotopic investigation of their effects on the Earth's oldest oceanic crustal sequence. Geochim. Cosmochim. Acta v. 66, p. 467–486.

Hoffmann, J.E., Nagel, T.J., Münker, C., Næraa, T., Rosing, M.T., 2014 Constraining the process of Eoarchean TTG formation in the Itsaq Gneiss Complex, southern West Greenland. Earth Planet. Sci. Lett, v. 388, p. 374-386.

Kemp, A., Whitehouse, M., Vervoort, J., 2019. Deciphering the zircon Hf isotope systematics of Eoarchean gneisses from Greenland: Implications for ancient crust-mantle differentiation and Pb isotope controversies. Geochimica et Cosmochimica Acta v. 250, p. 76-97.

Klemme, S., Günther, D., Hametner, K., Prowatke, S., Zackl, T. 2006. The partitioning of trace elements between ilmenite, ulvospinel, armalcolite and silicate melts with implications for the early differentiation of the moon. Chemical Geology v. 234, p. 251–263

Polat, A., Hofmann, A.W., Münker, C., Regelous, M., Appel, P.W.U., 2003. Contrasting geochemical patterns in the 3.7–3.8 Ga pillow basalt cores and rims, Isua greenstone belt, Southwest Greenland: implications for post-magmatic alteration processes. Geochim. Cosmochim. Acta v. 67, p. 441–457.

Polat, A., Hofmann, A.W., 2003. Alteration and geochemical patterns in the 3.7–3.8 Ga Isua greenstone belt, West Greenland. Precambrian Research, v. 126, p. 197-218.

Rollinson, H.R., 2003. Metamorphic history suggested by garnet-growth chronologies in the Isua Greenstone Belt, West Greenland. Precambrian Research, v. 126, p. 181-196.

Rollinson, H.R., Pease, V., 2021. Using Geochemical Data to understand geological processes (2nd Edn). Cambridge University Press, 346 p.

Szilas, K., Kelemen, P.B., Rosing, M.T., 2015. The petrogenesis of ultramafic rocks in the >3.7 Ga Isua supracrustal belt, southern West Greenland: Geochemical evidence for two distinct magmatic cumulate trends. Gondwana Research, v. 28, p. 565-580.

Tateno, S., Hirose, K., Sakata, S., Yonemitsu, K., Ozawa, H., Hirata, T., 2018. Melting phase relations and element partitioning in MORB to lowermost mantle conditions. Journal of Geophysical Research: Solid Earth, 123. https://doi.org/10.1029/2018JB015790

van de Locht, J., Hoffmann, J.E., Rosing, M.T., Sprung, P., Munker, C., 2020. Preservation of Eoarchean mantle processes in ~3.8 Ga peridotite enclaves in the Itsaq Gneiss Complex, southern West Greenland. Geochimica et Cosmochimica Acta, v. 280, p. 1-25